

Document downloaded from the institutional repository of the University of Alcalá: <http://dspace.uah.es/dspace/>

This is a postprint version of the following published document:

Tejedor, J., Martins, H.F., Piote, D., Macias-Guarasa, J., Pastor-Graells, J., Martin-Lopez, S., Corredera, P., De Smet, F., Postvoll, W., Gonzalez-Herraez, M., 2016, " Toward Prevention of Pipeline Integrity Threats Using a Smart Fiber-Optic Surveillance System", Journal of Lightwave Technology, v.34, n.19, pp. 4445-4453.

Available at <http://dx.doi.org/10.1109/JLT.2016.2542981>

© 2016 IEEE. "Personal use of this material is permitted. Permission from IEEE must be obtained for all other uses, in any current or future media, including reprinting/republishing this material for advertising or promotional purposes, creating new collective works, for resale or redistribution to servers or lists, or reuse of any copyrighted component of this work in other works."

*(Article begins on next page)*



This work is licensed under a

Creative Commons Attribution-NonCommercial-NoDerivatives  
4.0 International License.

# Towards Prevention of Pipeline Integrity Threats using a Smart Fiber Optic Surveillance System

Javier Tejedor, Hugo F. Martins, Daniel Piote, Javier Macias-Guarasa, *Member, IEEE*, Juan Pastor-Graells, Sonia Martin-Lopez, Pedro Corredera, Filip De Smet, Willy Postvoll, and Miguel Gonzalez-Herraez

**Abstract**—This paper presents the first available report in the literature of a system aimed at the detection and classification of threats in the vicinity of a long gas pipeline. The system is based on phase-sensitive optical time domain reflectometry ( $\phi$ -OTDR) technology for signal acquisition and pattern recognition strategies for threat identification. The system operates in two different modes: (1) machine+activity identification, which outputs the activity being carried out by a certain machine, and (2) threat detection, aimed at detecting threats no matter what the real activity being conducted is. Different strategies dealing with position selection and normalization methods are presented and evaluated using a rigorous experimental procedure on realistic field data. Experiments are conducted with 8 machine+activity pairs, which are further labeled as threat or non-threat for the second mode of the system. The results obtained are promising given the complexity of the task and open the path to future improvements towards fully-functional pipeline threat detection systems operating in real conditions.

**Index Terms**—Pipeline integrity threat monitoring, Distributed Acoustic Sensing, Fiber optic systems,  $\phi$ -OTDR

## I. INTRODUCTION

**P**IPELINE transmission is by far the most sustainable and safest transmission method to transport energy sources from the producing facilities to the various end-users. Special attention is paid by the transmission system operators, to ensure that these infrastructures are safely operated in order to prevent potential accidents [1], [2]. Since most incidents involving natural gas transmission infrastructures occur when pipelines are damaged by third party works in their vicinity, there is a need for cost-effective solutions allowing for continuous monitoring of potential threats to the pipeline integrity. Distributed Acoustic Sensing (DAS) technology is specially well suited for this task [3]–[5].

Within DAS technology, the use of vibration-based sensing to monitor activities near a pipeline represents a promising solution as it can detect the vibration associated to potentially dangerous activities, so that a preventive action can be undertaken. If we also add pattern recognition strategies (PRS) to further classify the sensed vibration into a set of relevant activities, we can increase the cost-effectiveness of the system, as the number of false alarms can be significantly reduced.

J. Tejedor, J. Macias-Guarasa, J. Pastor-Graells, S. Martin-Lopez, and M. Gonzalez-Herraez are with the Department of Electronics, University of Alcalá, Spain.

H.F. Martins and D. Piote are with FOCUS S.L., Spain.

P. Corredera is with Instituto de Optica, CSIC, Spain.

F. De Smet is with Fluxys Belgium S.A.

W. Postvoll is with Gassco AS, Norway.

Phase-sensitive Optical Time Domain Reflectometry ( $\phi$ -OTDR) has been demonstrated to be a reliable distributed fiber optic acoustic sensing technology and has been extensively researched, mainly in the context of long-perimeter intrusion monitoring. Conventional  $\phi$ -OTDR-based sensors can reach sensing ranges of a few tens of kilometers, with spatial resolutions of a few meters and have been demonstrated to provide enough sensitivity to allow the detection of people walking over a buried fiber [3]. With the use of distributed optical amplification, sensing ranges above 100 kilometers have been demonstrated [4]–[7]. As for the detection bandwidth, this is limited by the fiber length, and for short distances (less than one kilometer), vibrations up to 40 kHz have been detected [8]. Post-processing denoising methods have also been applied to improve the Signal-to-noise ratio (SNR) and therefore the limits of detection [7], [9]–[11].

Most of the  $\phi$ -OTDR-based reported works rely on directly measuring changes in the optical trace or are based on energy to detect perturbations, without employing more advanced techniques. From the few works that employ pattern classification, these present the following issues: no real classification is conducted [12], no classification results are reported [13], [14], the classification strategy is not presented [15], the sensing system is very close to the sensed area [12], the sensed area is small (20-meter long [16] and 44-meter long [12]), no enough details of the experimental setup (training and testing conditions, recording protocol, etc.) are given [14]–[17], or no real field data are used [16]. Additionally, the classification tasks in these works only deal with three classes at most.

Regarding the general task of classifying different types of vehicles/machinery, significant research has also been conducted by employing different sensing systems, with various strategies for feature extraction and classification [18]–[24]. All these works differ from our proposal in the fundamental fact that the sensing method is based on a linear transduction mechanism between the vehicle physical effects (acoustic or seismic) and the acquired signal, while in  $\phi$ -OTDR-based systems, the transduction function is intrinsically and inherently non-linear, except for very small perturbations. Additionally, the classification tasks in these works only deal with between two and six classes at most.

In this paper, we present (to the best of our knowledge) the first published report on a pipeline integrity threat detection and identification system that employs DAS+PRS technology and is evaluated on realistic field data, showing promising results in terms of accuracy, and thus its potential for real

world applications. To do so, the system supports two operational modes: (1) The *machine+activity* identification mode identifies the activity and the machine that is conducting the activity along the pipeline. (2) The *threat* detection mode directly identifies if the activity is a threat or not. This is also the first system that is set up for real time monitoring and classification of different types of (potentially harmful or not) activities occurring close to a long pipeline, and whose results are based on a rigorous experimental setup and an objective evaluation procedure with standard and clearly defined metrics.

The whole system is being developed under a GERG (The European Gas Research Group) supported project titled PIT-STOP (Early Detection of Pipeline Integrity Threats using a SmarT Fiber-Optic Surveillance System). Compared with our previous work [25], this paper extends the system with the machine+activity identification mode, and compares two signal normalization and selection methods.

The paper is organized as follows: Section II introduces the DAS system used for signal acquisition and Section III describes the pipeline integrity threat detection system. The experimental procedure is presented in Section IV and the experimental results are discussed in Section V. Finally, the conclusions are drawn in Section VI along with some lines for future work.

## II. DISTRIBUTED ACOUSTIC SENSING SYSTEM

### A. System Description

The distributed acoustic sensing system is a commercially available  $\phi$ -OTDR-based sensor (named FINDAS) manufactured and distributed by FOCUS S.L. [26]. A detailed description of the FINDAS underlying technology ( $\phi$ -OTDR) can be found in [8].

In the present work, the FINDAS sensor has an (optical) spatial resolution of 5 meters (readout resolution of 1 meter) and a typical sensing range of up to 45 kilometers, using standard Single-Mode Fiber (SMF). Distributed optical amplification was not used. The FINDAS sensor was connected to a standard SMF, which had been previously installed parallel along the pipeline to be monitored. A sampling frequency of  $f_s = 1085$  Hz was used for signal acquisition, given the experimental setup. The FINDAS sensor is used to continuously monitor vibrations along the pipeline. Since the fiber does not follow a tight parallel path along the pipeline, and in some points there were fiber rolls (for maintenance purposes), a calibration between fiber distance and geographical location was carried out.

### B. Signal Behavior

The physical process involved in the signal measurement along with the mechanical properties related to each sensed location affect the signal characteristics in a great extent.

Firstly, the propagation of ground vibrations depends mainly on the machinery distance, the soil characteristics (dry or wet, compact or soft, earth or concrete, etc.), and the mechanical coupling of the fiber to the pipe enclosure. Therefore, the acoustic signal from a certain activity can present variations from one location to another. Additionally, the background

noise can also vary for different locations (due to the proximity of roads, factories, etc.).

Secondly, as mentioned in Section I, the transduction function of a  $\phi$ -OTDR-based sensor is non-linear, and it is particularly relevant in the case of strong perturbations, as in the scenario considered in this work. In addition, owing to the random nature of a  $\phi$ -OTDR signal, specific points randomly distributed along the fiber (the so-called fading points [8]) can present low, or even null sensitivity to vibrations. In practice, by analyzing several consecutive points, it will be ensured that a certain acoustic signal is received from a given location, but the sensitivity of the fiber can vary locally from one point to another.

Finally, due to the fiber losses, the optical power received from a fiber location at a distance of  $d_m$  meters from the beginning (i.e., input) of the fiber, denoted as  $P(d_m)$  – and therefore the amplitude of the measured signals – will exhibit an exponential decay along the fiber. The fiber attenuation coefficient is given by  $\alpha \approx 0.0002\text{dB/m}$  at the operating laser wavelength (1550 nm). For a given optical power at the input of the fiber  $P(0)$ ,  $P(d_m)$  will be  $P(d_m) = P(0) \cdot 10^{(-2 \cdot d_m \cdot \alpha / 10)}$ . Considering the full round-trip of the fiber light, this implies a 3 dB decay for every 7.5 kilometers, so that the effects of the optical losses will be relevant for distances of tens of kilometers.

## III. PIPELINE INTEGRITY THREAT DETECTION SYSTEM

The pipeline integrity threat detection system operates in two different modes: *machine+activity identification* and *threat detection*. In the first mode, the input acoustic signal acquired by FINDAS is classified as corresponding to a certain machine+activity pair, among those considered in the task. In the threat detection mode, the signal is classified as threat or non-threat. The first mode is suitable for cases where both the machine and the activity being conducted must be known. The second mode is suitable for cases in which just the occurrence of a threat to the pipeline must be known.

The system is based on a pattern recognition core and integrates three different stages: (1) feature extraction, which reduces the high dimensionality present in the acoustic raw data, while retaining a high discriminative power, (2) feature vector normalization, to compensate for variabilities in the signal acquisition process and the sensed location, and (3) pattern classification, which classifies each feature vector into the most likely class (*machine+activity pair* in the machine+activity identification mode, or *threat/non-threat* in the threat detection mode). These three stages are described next.

### A. Feature Extraction

The feature extraction employs a Short-Time Fast Fourier Transform (ST-FFT) to calculate energy over frequency bands for each acoustic frame (a signal window at any given time), which are used as the base feature vector components.

The full base feature vector calculated at a given fiber position located at a distance of  $d_m$  meters will be  $\mathbf{x}_m = (e_{m0}, e_{m1}, \dots, e_{mP})$ , where  $e_{mi}$  is the energy calculated at position  $d_m$  for band  $i$ , and  $P$  bands are calculated

TABLE I: Recording location details.

	LOC1	LOC2	LOC3	LOC4	LOC5	LOC6
<b>Distance from FINDAS (km)</b>	22.24	22.49	23.75	27.43	27.53	34.27
<b>Soil condition</b>	Grass & clay in agricultural field	Grass in agricultural field	Concrete, grass & clay Next to public street Private house nearby	Wet clay in agricultural field	Clay in agricultural field	Grass in forest
<b>Weather condition</b>	Sunny/cloudy	Sunny	Sunny	Rainy	Cloudy	Sunny

for the considered bandwidth  $f \in [f_0, f_{BW}]$ , with  $f_0$  and  $f_{BW}$  being the initial and final frequencies respectively, and  $f_{BW} \leq \frac{f_s}{2}$ . For the frequency band limit calculation, a standard Mel scale has been used [27].

### B. Feature Vector Normalization

Given the considerations in Section II-B, feature normalization is especially important in this application in which we face strong differences due to the signal acquisition process and the sensed location. Not all the variabilities can be properly handled with normalization strategies, but we can effectively reduce some of them.

The two main normalization strategies that have been applied on the base feature vectors are related to the sensed location and are described below.

1) *Fiber loss compensation normalization*: The objective of this normalization is to compensate for the signal's amplitude exponential decay with the distance due to fiber losses. For this, a normalization factor  $\eta_m$  in a certain position  $d_m$  has been applied to each acoustic signal, so that its amplitude along the fiber is normalized with respect to the amplitude of the signal at the fiber entrance (thus eliminating the attenuation effect shown in Section II-B). This normalized vector will be referred to as  $\mathbf{x}_m^\eta$ .

2) *Sensitivity-based normalization*: To compensate for this effect so that we obtain signals of equivalent sensitivity along the fiber, we will assume that the variable sensitivity is frequency independent. Thus, the variability will equally affect all frequency components, and a normalization factor based on the energy of the spectral content above the considered bandwidth (where no relevant information is to be found) will be applied. The normalized feature vector in this case will be referred to as  $\mathbf{x}_m^\beta$ .

### C. Pattern Classification

Our pattern classification system is based on Gaussian Mixture Models (GMMs), which have been extensively used for classification and clustering in different research areas related to speech [28], image [29], and video [30] recognition, among others.

The motivation of using GMMs relies on the fact that they require limited amount of resources and have a good pattern matching performance [31]. In addition, GMMs provide a straightforward mechanism by which a linear combination of Gaussian basis functions can be employed to represent a large class of sample distributions (i.e., *training* and *testing* data).

So, given a GMM  $\lambda$ , the probability that vector  $\mathbf{x}$  belongs to the class represented by  $\lambda$  can be easily derived and will be referred to as  $p(\mathbf{x}|\lambda)$ .

Given a subset of acoustic files recorded for a given class  $k$  (the *training* subset), model training is carried out to estimate the parameters of each GMM  $\lambda_k$ . Maximum likelihood model parameters are estimated from the Expectation-Maximization algorithm [32]. Once the models have been trained, classification is carried out on an independent subset (the *testing* subset), to find the class model  $\hat{c}$  which has the maximum *a posteriori* probability for a given input feature vector  $\mathbf{x}$  as follows:

$$\hat{c} = \underset{k}{\operatorname{argmax}} \frac{p(\mathbf{x}|\lambda_k)p(\lambda_k)}{p(\mathbf{x})} = \underset{k}{\operatorname{argmax}} \{p(\mathbf{x}|\lambda_k)\}, \quad (1)$$

where we have applied Bayes' rule, and assume a uniform a priori probability for every class (i.e.,  $p(\lambda_k) = 1/C$ ).

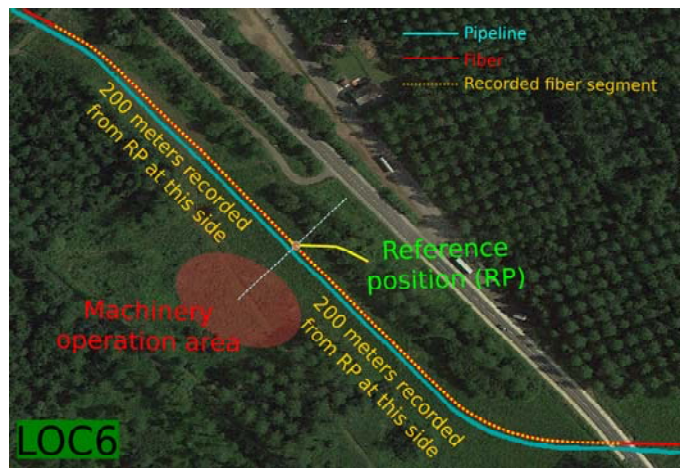


Fig. 1: Recording scenario: Real example at LOC6.

## IV. EXPERIMENTAL PROCEDURE

### A. Signal Recording and Labeling

An active gas transmission pipeline operated by Fluxys Belgium S.A. was used as the recording scenario, thus operating in a real scenario. Activities nearby the pipeline were sensed by monitoring an optical fiber cable installed about 0.5 meters from the pipeline and parallel to it along several kilometers.

To deal with different acoustic and environmental variabilities, different activities from different machines were recorded by FINDAS during four consecutive days at six different locations (LOC1 through LOC6) with varying (optical fiber) distances from the sensing equipment, and varying soil and weather conditions (details are provided in Table I). These differences in terms of location properties make possible to test the system under different environments and soil conditions

TABLE II: Experimental database. ‘Big excavator’ is a 5 ton Kubota KX161-3. ‘Small excavator’ is a 1.5 ton Kubota KX41-3V.

Machine	Activity	Duration (in seconds)						Total	Threat/Non-threat
		LOC1	LOC2	LOC3	LOC4	LOC5	LOC6		
Big excavator	Moving along the ground	1100	1100	3540	1740	1620	4160	13260	Non-threat
	Hitting the ground	120	140	240	220	80	260	1060	Threat
	Scrapping the ground	460	460	920	620	200	580	3240	Threat
Small excavator	Moving along the ground	600	500	1700	820	820	1660	6100	Non-threat
	Hitting the ground	200	180	220	220	80	240	1140	Threat
	Scrapping the ground	420	340	780	360	180	520	2600	Threat
Pneumatic hammer	Compacting ground	660	0	580	1320	0	1320	3880	Non-threat
Plate compactor	Compacting ground	740	0	740	1240	0	1680	4400	Non-threat

which may greatly affect the final system performance. Note also that at every location, the fiber enclosure pipe is physically deployed in different ways (physical coupling, enclosure depth, etc.). In addition, to improve the reliability of the system performance estimation, and for a better system generalization on unseen data, the same machine+activity pairs were recorded every day in different locations and times.

In the recording protocol for each location (see Figure 1), the first step was defining a *reference meter* position. This was chosen manually as the closest to the center of the operation area with good sensitivity, by real time monitoring of the fiber response while a well defined activity was being carried out (in this case a plate compactor carrying out the compacting ground activity was used). FINDAS equipment was employed to select this reference position. Taking this reference position as the middle position for the recordings, 400 meters were recorded (with a 1 meter readout resolution), 200 meters at each side of the reference position, so that 400 acoustic traces were generated for each of the recorded activities (which are split in chunks of 20 seconds for better signal management and storage).

Four different machines performing different activities were used to build 8 machine+activity pairs to be classified (in the machine+activity identification mode of the pipeline integrity threat detection system): a 5 ton Kubota KX161-3 (moving along the ground, hitting the ground, scrapping the ground), a 1.5 ton Kubota KX41-3V (moving along the ground, hitting the ground, scrapping the ground), a pneumatic hammer (compacting ground), and a plate compactor (compacting ground). These machine+activity pairs were further labeled as *threat* or *non-threat* depending on whether they were considered potentially harmful to the integrity of the pipeline (to be used in the threat detection mode of the system). As can be seen in Table II, four pairs are considered as *threat*: Kubota KX161-3 – hitting and scrapping the ground–, and Kubota KX41-3V – hitting and scrapping the ground–. The remaining 4 pairs are considered as *non-threat*. Therefore, the machine+activity identification mode involves 8 different classes and the threat detection mode involves 2 different classes.

### B. Database Description

The acoustic database for training and testing was built from the machine+activity pairs recorded in different locations, as described in Section IV-A. Full details of the recorded data are presented in Table II, where the duration per location and the threat/non-threat label corresponding to each machine+activity

pair are presented. Duration refers to the material available for a single meter, but take into account that there are 400 simultaneous acoustic traces recorded at any given time.

### C. Preliminary Experiments

Given the lack of previous work of the scale approached in this work, we devoted a lot of effort to thoroughly design and evaluate different methodologies and strategies to successfully face the classification task, considering all the system modules, aiming to deciding a suitable system configuration.

Particularly relevant were the studies related to the actual effects of location variability. The careful design of the database, with samples for several machines carrying out various activities across several locations, allowed us to conduct single-site (i.e., using data for training and testing from the same location), cross-site (i.e., using data for training from one location, and testing from a different location), and multi-site (i.e., using data for training from several locations, and testing on a different location) evaluation experiments.

The main conclusion from these experiments was that modeling location variability is extremely relevant to obtain good performance. To provide a quantitative comparison for preliminary experiments, the machine+activity performance rates for single-site classification were around 40%, and they dropped to around 18% when cross-site evaluation was carried out.

So, as it is impossible to gather data from every possible location along a pipeline (to carry out single-site evaluation), selecting a reasonable number of locations for multi-site training is a must.

Much attention was also given to study the effect of the control parameters for the algorithms used: bandwidth, number of frequency bands, frequency scaling, number of GMM components, and acoustic trace selection, among others.

### D. System Configuration

The bandwidth of the acquired acoustic signals covers frequencies up to 542.5 Hz, but experiments were carried out by analyzing frequencies up to 100 Hz, since frequencies above 100 Hz do not convey meaningful information. The low limit of the spectral range was set to 1 Hz, since the window size in the ST-FFT expands one second. The relevant parameters related to the energy-in-bands computation in the feature extraction are: the acoustic frame size (which in the system is set to 1 second), the acoustic frame shift (set to 5 milliseconds), the number of FFT points (set to 8192) for

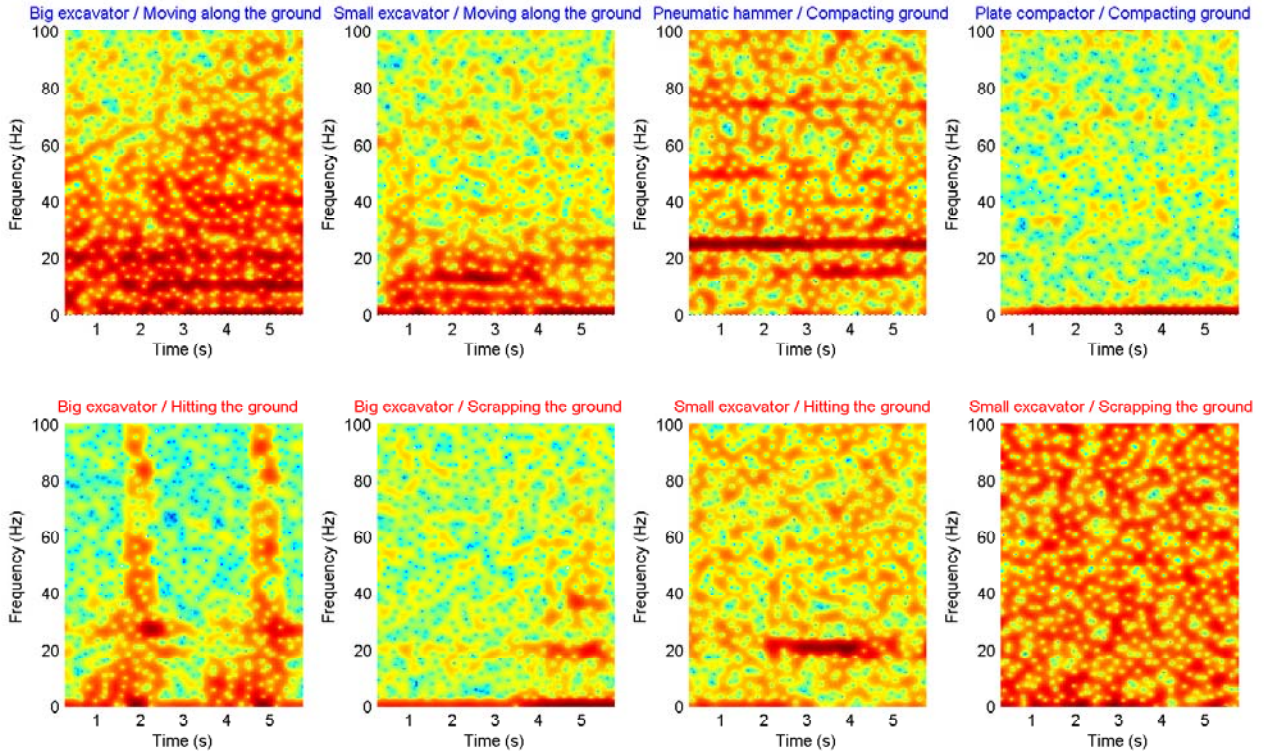


Fig. 2: Examples of spectrograms of the signals generated by different machine+activity pairs. The top row corresponds to *non-threat* activities and the bottom row corresponds to *threat* activities.

the Short-Time Fast Fourier Transform, and the number of frequency bands that defines the number of components in the feature vectors (set to  $P = 100$ ). These values were chosen based on their best performance in preliminary experiments.

A single GMM component per class has been used for model training in the pattern classification stage, as a baseline setup to allow for robust training and easier generalization.

To increase the statistical significance of the system performance estimation, the experiments are carried out using a leave-one-out cross-validation (CV) strategy, on a location basis. Since data were recorded in 6 different locations, the CV comprises 6 folds, where the data recorded in all the locations except one were used for training, and the evaluation was done on data of the unused location (thus ensuring full independence between the training and testing subsets).

Classification is conducted on a frame-by-frame basis. Therefore, a feature vector ( $\mathbf{x}_m$ ,  $\mathbf{x}_m^\eta$ , or  $\mathbf{x}_m^\beta$ ) is calculated for each 1 second frame within every 20 second length recorded file. All the vectors are used in the pattern classification stage, either as training or testing data. Therefore, given the feature extraction parameters, there are 415 feature vectors for each recorded file.

#### E. Highest Energy Meter Selection

During preliminary experiments, it became clear the severe effect of the strong sensitivity variations across time and location, even for acoustic traces in contiguous positions.

Therefore, we decided to evaluate a strategy to select the sensed position (different to the middle position) as that with the highest energy to be used in the training and testing procedures. The energy calculation is done with the same parameters as those used in the feature extraction (see Section IV-D).

#### F. Evaluation Metrics

Classification accuracy has been the main metric to evaluate the system performance both for the machine+activity identification and threat detection modes. For any given class, the classification accuracy is defined as the ratio between the number of correctly classified testing frames and the total number of testing frames for the given class. The overall classification accuracy is then computed as the ratio between the number of correctly classified testing frames and the total number of testing frames.

Additionally, and to provide a full picture of the classification performance, we are also showing:

- For the machine+activity identification mode: The full confusion matrix, this is, a table showing the percentage of testing frames of a given class that have been classified as any of the considered classes, being it a powerful method for performance analysis.
- For the threat detection mode: The threat detection rate (which corresponds to the percentage of threat testing frames that are classified as threat, usually referred to

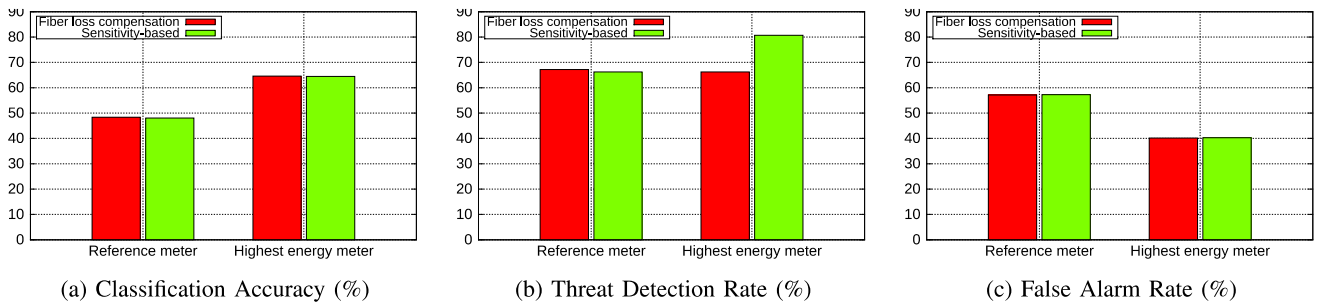


Fig. 3: Results for the threat detection mode.

as *true positives*), and the false alarm rate (which corresponds to the percentage of non-threat testing frames that are classified as threat, usually referred to as *false positives*).

## V. EXPERIMENTAL RESULTS

### A. Signal Analysis

An initial analysis was carried out aiming at checking whether meaningful and discriminative patterns for each machine+activity pair exist. To do so, spectrograms were computed from randomly selected acoustic files. These acoustic files are those corresponding to a highest energy meter for a given machine+activity pair in a certain location according to the 20-second length duration of each acoustic file in the database. To provide a general idea on the signal characteristics, some examples of these spectrograms are shown in Figure 2, where it can be seen that the signals have a high level of noise and that, in general, each machine+activity pair exhibits a reasonably consistent spectral behavior, hence allowing for the use of pattern classification strategies.

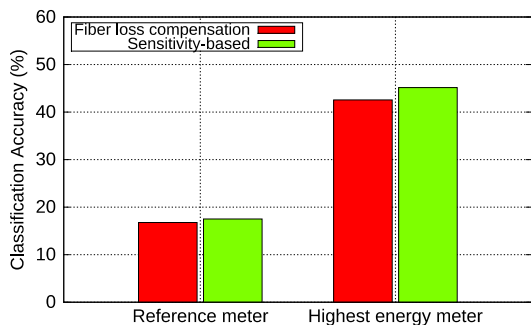


Fig. 4: Results for the machine+activity identification mode.

### B. Results and Discussion

Figure 3 presents the results obtained with the two normalization methods and the two fiber meter selection methods for the threat detection mode of the pipeline integrity threat detection system. In the same way, results for the machine+activity identification mode of the system are presented in Figure 4.

At first sight, the performance rates may seem low, but we have to take into account the complexity of the task (refer to Section II-B for details), and that this proposal is just a

first step towards threat detection dealing with fully realistic conditions.

From Figures 3 and 4, it is clear that the classification accuracy is much better with the use of the highest energy meter than with the use of the reference meter. Paired  $t$ -tests [33] show that this improvement is statistically significant for the fiber loss compensation normalization ( $p < 10^{-38}$ ) and the sensitivity-based normalization ( $p < 10^{-42}$ ) in the machine+activity identification mode. For the threat detection mode, the improvement in terms of classification accuracy is also statistically significant for both normalization methods ( $p < 10^{-33}$ ). The threat detection rate and the false alarm rate also improve with the use of the highest energy meter. Paired  $t$ -tests show that this improvement is statistically significant for both normalization methods ( $p < 10^{-26}$ ). This is because the highest energy meter agglutinates more discriminative information of the machine+activity pair and threat/non-threat represented in the acoustic signal. However, selecting the reference meter degrades the system performance since fixing the evaluated position does not allow taking into account sensitivity variations along time. Since the threat/non-threat classes are built from these same machine+activity pairs, the same explanation holds for the threat detection mode.

In terms of the best normalization method, the results are not that clear. For the machine+activity identification mode (Figure 4), the sensitivity-based normalization significantly outperforms the fiber loss compensation normalization ( $p < 10^{-19}$ ). Contrary, for the threat detection mode (Figure 3), both methods are almost equivalent, and only the fiber loss compensation normalization weakly outperforms the sensitivity-based normalization for the overall classification accuracy ( $p < 0.04$ ) and for the false alarm rate ( $p < 0.08$ ). In the threat detection rate, a paired  $t$ -test did not show any statistical difference between both normalization methods ( $p \approx 0.6$ ).

With two possible classes (threat/non-threat in the threat detection mode), the normalization based on the fiber position is enough to get the best performance. This means that the simple normalization considering only the fiber position is good enough for this binary classification task. However, for the more complex machine+activity identification mode, the sensitivity-based normalization is preferable. We consider this is due to the fact that a much more informed normalization strategy helps the system to sort out a wider variety of energy conditions, thus helping to train more robust models.

TABLE III: Confusion matrix of the Sensitivity-based normalization method and highest energy-based meter selection for the machine+activity identification mode (numbers between brackets indicate the number of frames in each machine+activity pair).

			Recognized class							
			Big excavator			Small excavator			Pneumatic Hammer	Plate Compactor
			[180870] Moving	[68020] Hitting	[90281] Scrapping	[109094] Moving	[55429] Hitting	[94043] Scrapping	[74171] Compacting	[68452] Compacting
Real class	Big excavator	[275145] Moving	49.05	13.79	12.77					
		[21995] Hitting	19.95	20.11	20.42			15.63		
		[67230] Scrapping			26.03			20.35		
	Small excavator	[126575] Moving	13.22			50.50				
		[23655] Hitting			15.35		13.78	28.04	16.10	
		[53950] Scrapping			16.78		14.25	30.22	16.06	
	Pneumatic hammer	[80510] Compacting						71.84		
	Plate Compactor	[91300] Compacting					22.40		39.51	

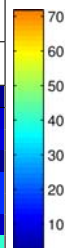


Table III presents the confusion matrix for the machine+activity identification mode (we have removed the values below chance ( $1/8 = 12.5\%$ ) to ease the visualization and analysis).

It is clear that the values in the diagonal are all above chance. The best recognized classes are the moving activities carried out by the excavators (probably due to the fact that their training subset sizes were the highest ones, thus generating more robust models), the pneumatic hammer (which had the clearest and best defined spectral behavior), and the plate compactor (also with a consistent spectral content).

It can also be seen that confusion is high within all the activities carried out by the big excavator, and also by the small excavator. These confusions are reasonable, given that the machine is the same and the engine vibrations will be present during all the activities. Within the excavator activities, confusions are higher for the hitting ones. This may be due to the fact that the hitting activities have the smallest amount of training data (see Table II). Having a small number of training data is an important and well-known issue when building a pattern recognition system, which derives in a less robust GMM, thus decreasing its performance rates. Hitting and scrapping activities also exhibit confusion, as the scrapping activity also includes hitting when the shovel contacts the ground.

Confusions between the activities carried out by the big and small excavators mainly happen for the scrapping activity, which is also acoustically similar for both machines.

The hitting and scrapping activities carried out by the small excavator are also confused with the plate compactor (presumably due to the small amount of training data of the small excavator+hitting and small excavator+scrapping classes, and the previously mentioned similarity between scrapping and hitting).

Hitting and scraping activity performance is also degraded due to the fact that they comprise different acoustic behaviors (moving up the shovel, moving it down, hitting, scrapping, etc.) but only one GMM component is used, thus making it more difficult to model them accurately. Their performance could also be improved if multiple components per GMM are used.

## VI. CONCLUSIONS AND FUTURE WORK

This paper has presented, to the best of our knowledge, the first report on a pipeline integrity threat detection system

that employs a  $\phi$ -OTDR fiber optic-based sensing system for data acquisition. Two different modes have been set in the system: machine+activity identification and threat detection. The machine+activity identification mode aims at identifying the machine+activity pair that is acting on the pipeline, which can be next employed to decide if this constitutes a threat or not for the integrity of the pipeline. The threat detection mode focuses on direct identification of the possible threats that can occur along the pipeline, no matter the reason by which each threat was caused.

An evaluation and comparison of different strategies dealing with position selection and normalization methods has been presented, using a rigorous experimental procedure on realistic field data. The results presented in this paper exhibit good performance in terms of threat detection, since 8 out of 10 threat activities are correctly recognized, and 4 out of 10 times the system presents a false positive. For machine+activity identification, given the complexity of the task (8 classes), the system also obtains reasonable performance.

Even when we can say that the results are promising, there is still a lot of work to do, especially in what respect to evaluating the approach for a wider range of machinery activities and adopting alternative and more sophisticated classification strategies. The need to deal with real machinery activities makes the evaluation more difficult than in related precedents (such as temperature and strain studies), but the close collaboration between implicated industry and academia will surely alleviate the difficulties. The lessons learnt indicate that the DAS+PRS approach is suitable to provide realistic solutions that complement the existing surveillance methods. This work has also established a thorough experimental methodology which ensures that future contributions will need to be validated by a rigorous evaluation procedure to accurately assess the validity of the proposals.

## ACKNOWLEDGMENTS

This work was mainly supported by three GERG partners (Fluxys Belgium, Statoil, and Gassco) under project PIT-STOP. In addition, some authors were supported by funding from the European Research Council through Starting Grant UFINE (Grant no. 307441), the Spanish ‘‘Plan Nacional de I+D+i’’ through projects TEC2012-37958-C02-01, TEC2012-37958-C02-02, TEC2011-27314, TEC2013-45265-R, and TIN2013-47630-C2-1-R, the regional programs SIN-



FOTONCM: S2013/MIT-2790 and EDISON (CCG2014/EXP-072) funded by the “Comunidad de Madrid”, and INTERREG-ECOAL project. HFM acknowledges funding through the FP7 ITN ICONE program, gr. #608099 funded by the European Commission. JPG acknowledges funding from the Spanish Ministry of Economy and Competivity through an FPI contract. SML acknowledges funding from the Spanish Ministry of Science and Innovation through a “Ramón y Cajal” contract.

## REFERENCES

- [1] P. S. Trust, “Nationwide data on reported incidents by pipeline type (gas transmission, gas distribution, hazardous liquid),” 2004, <http://pstrust.org/about-pipelines1/stats/accident/>, Last access November 2015.
- [2] E. G. P. I. D. G. (EGIG), “9<sup>th</sup> egig-report on gas pipeline incidents (1970-2013),” Tech. Rep., 2015.
- [3] J. C. Juárez, E. W. Maier, K. N. Choi, and H. F. Taylor, “Distributed fiber-optic intrusion sensor system,” *Journal of Lightwave Technology*, vol. 23, no. 6, pp. 2081–2087, 2005.
- [4] H. F. Martins, S. Martín-López, P. Corredera, M. L. Filograno, O. Frazão, and M. González-Herráez, “Phase-sensitive optical time domain reflectometer assisted by first-order Raman amplification for distributed vibration sensing over > 100 km,” *Journal of Lightwave Technology*, vol. 32, no. 8, pp. 1510–1518, 2014.
- [5] Z. Wang, J. Zeng, J. Li, M. Fan, H. Wu, F. Peng, L. Zhang, Y. Zhou, and Y. Rao, “Ultra-long phase-sensitive OTDR with hybrid distributed amplification,” *Optics Letters*, vol. 39, no. 20, pp. 5866–5869, 2014.
- [6] H. F. Martins, S. Martín-López, P. Corredera, J. D. Ania-Castañón, O. Frazão, and M. González-Herráez, “Distributed vibration sensing over 125 km with enhanced SNR using phi-OTDR over a URFL cavity,” *Journal of Lightwave Technology*, vol. 33, no. 12, pp. 2628–2632, 2015.
- [7] F. Peng, H. Wu, X.-H. Jia, Y.-J. Rao, Z.-N. Wang, and Z.-P. Peng, “Ultra-long high-sensitivity  $\phi$ -OTDR for high spatial resolution intrusion detection of pipelines,” *Optics Express*, vol. 22, no. 11, pp. 13 804–13 810, 2014.
- [8] H. F. Martins, S. Martín-López, P. Corredera, M. L. Filograno, O. Frazão, and M. González-Herráez, “Coherent noise reduction in high visibility phase sensitive optical time domain reflectometer for distributed sensing of ultrasonic waves,” *Journal of Lightwave Technology*, vol. 31, no. 23, pp. 3631–3637, 2013.
- [9] Z. G. Quin, L. Chen, and X. Y. Bao, “Wavelet denoising method for improving detection performance of distributed vibration sensor,” *IEEE Photonics Technology Letters*, vol. 24, no. 7, pp. 542–544, 2012.
- [10] —, “Continuous wavelet transform for nonstationary vibration detection with phase-OTDR,” *Optics Express*, vol. 20, no. 18, pp. 20 459–20 465, 2012.
- [11] T. Zhu, X. Xiao, Q. He, and D. Diao, “Enhancement of SNR and spatial resolution in  $\psi$ -OTDR system by using two-dimensional edge detection method,” *Journal of Lightwave Technology*, vol. 31, no. 17, pp. 2851–2856, 2013.
- [12] C. Madsen, T. Baea, and T. Snider, “Intruder signature analysis from a phase-sensitive distributed fiber-optic perimeter sensor,” in *Proc. of SPIE*, vol. 6770, 2007, pp. 67 700K–1–67 700K–8.
- [13] H. Zhu, C. Pan, and X. Sun, “Vibration pattern recognition and classification in OTDR based distributed optical-fiber vibration sensing system,” in *Proc. of SPIE*, vol. 9062, 2014, pp. 906 205–1–906 205–6.
- [14] C. Conway and M. Mondanos, “An introduction to fibre optic intelligent distributed acoustic sensing (iDAS) technology for power industry applications,” in *Proc. of International Conference on Insulated Power Cables*, vol. A3.4, 2015, pp. 1–6.
- [15] H. Wu, Z. Wang, F. Peng, Z. Peng, X. Li, Y. Wu, and Y. Rao, “Field test of a fully distributed fiber optic intrusion detection system for long-distance security monitoring of national borderline,” in *Proc. of SPIE*, vol. 91579, 2014, pp. 915 790–1–915 790–4.
- [16] H. Wu, X. Li, Z. Peng, and Y. Rao, “A novel intrusion signal processing method for phase-sensitive optical time-domain reflectometry ( $\phi$ -OTDR),” in *Proc. of SPIE*, vol. 9157, 2014, pp. 91570–1–91570–4.
- [17] Q. Sun, H. Feng, X. Yan, and Z. Zeng, “Recognition of a phase-sensitivity OTDR sensing system based on morphologic feature extraction,” *Sensors*, vol. 15, pp. 15 179–15 197, 2015.
- [18] G. Jobin, M. Leena, and K. S. Riyas, “Vehicle detection and classification from acoustic signal using ANN and KNN,” in *Proc. of International Conference on Control Communication and Computing*, 2013, pp. 436–439.
- [19] J. Huang, Q. Zhou, X. Zhang, E. Song, B. Li, and X. Yuan, “Seismic target classification using a wavelet packet manifold in unattended ground sensors systems,” *Sensors*, vol. 13, pp. 8534–8550, 2013.
- [20] D. Li, K. D. Wong, Y. H. Hu, and A. M. Sayeed, “Detection, classification and tracking of targets in distributed sensor networks,” *IEEE Signal Processing Magazine*, vol. 19, no. 2, pp. 17–29, 2002.
- [21] C. Meesoorkho, S. Narayanan, and C. Raghavendra, “Collaborative classification applications in sensor networks,” in *Proc. of Sensor Array and Multichannel Signal Processing Workshop*, 2002, pp. 370–374.
- [22] Z. Xueyuan, Y. Xu, S. Enliang, L. Baoqing, and Y. Xiaobing, “A distance segmented classification algorithm for ground moving targets based on seismic-acoustic sensor arrays and parallel fuzzy classifier,” *Journal of Computational Information Systems*, vol. 8, no. 7, pp. 2789–2798, 2012.
- [23] M. Kandpa, V. K. Kakar, and G. Verma, “Classification of ground vehicles using acoustic signal processing and neural network classifier,” in *Proc. of International Conference on Signal Processing and Communication*, 2013, pp. 512–518.
- [24] C. Z. Jinghua Li and Z. Li, “Battlefield target identification based on improved grid-search SVM classifier,” in *Proc. of International Conference on Computational Intelligence and Software Engineering*, 2009, pp. 1–4.
- [25] H. F. Martins, D. Piote, J. Tejedor, J. Macias-Guarasa, J. Pastor-Graells, S. Martín-López, P. Corredera, F. D. Smet, W. Postvoll, C. H. Ahlen, and M. González-Herráez, “Early detection of Pipeline Integrity Threats using a Smart fiber-Optic surveillance system: The PIT-STOP project,” in *Proc. of SPIE*, vol. 9634, 2015, pp. 96 347X–1–96 347X–4.
- [26] F. S.L., “Fiber Network Distributed Acoustic Sensor (FINDAS),” 2015, <http://www.focustech.eu/FINDAS-MR-datasheet.pdf>, Last access November 2015.
- [27] S. B. Davis and P. Mermelstein, “Comparison of parametric representations for monosyllabic word recognition in continuously spoken sentences,” *Acoustics, Speech and Signal Processing, IEEE Transactions on*, vol. 28, no. 4, pp. 357–366, 1980.
- [28] Y. Zhang, M. Alder, and R. Togneri, “Using Gaussian mixture modeling in speech recognition,” in *Proc. of ICASSP*, 1994, pp. 613–616.
- [29] H. Permuter, J. Francos, and I. Jermyn, “A study of Gaussian mixture models of color and texture features for image classification and segmentation,” *Pattern Recognition*, vol. 39, no. 4, pp. 695–706, 2006.
- [30] T. Yu, C. Zhang, M. Cohen, Y. Ru, and Y. Wu, “Monocular video foreground/background segmentation by tracking spatial-color Gaussian mixture models,” in *Proc. of Workshop on Motion and Video Computing*, 2007, pp. 1–5.
- [31] Y. Kim, S. Jeong, D. Kim, and T. S. López, “An efficient scheme of target classification and information fusion in wireless sensor networks,” *Personal and Ubiquitous Computing*, vol. 13, no. 7, pp. 499–508, 2009.
- [32] G. Xuan, W. Zhang, and P. Chai, “EM algorithms of Gaussian mixture model and hidden Markov model,” in *Proc. of International Conference on Image Processing*, 2001, pp. 145–148.
- [33] H. A. David and J. L. Gunnink, “The paired t test under artificial pairing,” *The American Statistician*, vol. 51, no. 1, pp. 9–12, 1997.